THE BANDED TERRAIN ON THE HELLAS BASIN FLOOR, MARS: GRAVITY-DRIVEN FLOW NOT SUPPORTED BY NEW OBSERVATIONS H. Bernhardt[1], M. Ivanov[2], D. Reiss[1], H. Hiesinger[1], E. Hauber[3], J. D. Clark[1,4]
[1]Institut für Planetologie, Westfälische Wilhelms-Universität, Wilhelm-Klemm-Str. 10, 48149 Münster, Germany (h.bernhardt@uni-muenster.de), [2]Vernadsky Institute, Russian Academy of Sciences, Moscow, Russia, [3]Institut für Planetenforschung, Deutsches Zentrum für Luft- und Raumfahrt, Berlin, Germany, [4]School of Earth and Space Exploration, Arizona State University, Tempe, USA.

Introduction: The western Hellas basin floor on Mars hosts a complex landscape containing several unique landforms in close geographic association, e.g., the "honeycomb" and "banded" (or "taffy pull") terrains [e.g., 1-4]. Recent investigations concluded the honeycomb terrain to be truncated diapirs, possibly of salt or ice [3,5]. However, while periglacial features have been observed on the enigmatic banded terrain [1,3,6], its nature, formation, and thus its implications for the geologic, as well as climatic history of the Hellas basin remain largely unknown.

Data and methods: In order to resolve the textures of the banded and honeycomb terrains over their entire extents, we produced a 1:175,000 photogeologic map encompassing an area of ~159,700 km² between 50°E 33.4°S and 61.3°E 44.3°S on the west-northwestern Hellas basin floor (Fig. 1A). The mapping process was carried out on a purpose-built, seamless CTX [e.g., 7] mosaic alongside version 12 of the THEMIS-IR Day Global Mosaic [8] and the global MOLA DEM [9]. Local-scale observations, including multi-temporal investigations, were made using HiRISE [10] as well as MOC-NA [11] images. Based on the CTX mosaic and MOLA DTM, we also performed a grid mapping (2x2 km grid size) of the entire banded terrain to assess its relation to local slopes (Fig. 1B).

Observations: The characteristics of the banded terrain have been described in detail by [1,3,4]. In our map (Fig. 1A) it covers over 30,000 km² and is subdivided into two subtypes. The creviced type (light blue/grey) is a smooth surface dissected by curvilinear troughs ("inter-bands" [1]). The ridged type (navy blue) has a rougher surface and shows the same general texture, but produced by ridges with the same dimensions as the troughs. In some locations, ridged type areas appear to superpose creviced type areas. Individual bands appear to interact in both, brittle and ductile manners (e.g., HiRISE PSP_008269_1395 showing one band "breaking" through another, causing slab rotation). Comparisons of MOC-NA with HiRISE images taken up to 14 years apart show no discernible change within the banded terrain (e.g., collapse by de-volatilization). The banded terrain superposes the honeycomb terrain (e.g., partially filling several honeycomb cells) as well as the hummocky, more elevated interior formation of the Hellas basin. Along its transition to the lower "Hellas Planitia trough" in the northwestern basin, the material of the interior formation appears as elongate mesas embayed by banded terrain (dark blue in Fig. 1A). In many locations, band orientations are aligned to the mesas, or terminate on one side and continue on the other. Several large crater ejecta (yellow in Fig 1A; e.g., Beloha crater) superpose the banded terrain. In certain locations, e.g., at 57,66°E 35,67°S, ejecta appears to be dissected by bands of the underlying banded terrain.

According to our grid mapping (Fig. 1B) the orientation of bands does not seem to correlate with the local slope. All grid box categories (Fig. 1B inlets) are nearly equally abundant and distributed randomly, except within the honeycomb cells (circular arrangements dominant) and in the northernmost extents (lobate/slope-perpendicular arrangements dominant). In general, the banded terrain occurs across an elevation spectrum of almost 2 km, from -7667 m up to -5548 m (Fig. 1C). Within this spectrum, the creviced type follows a quasi-Gaussian distribution, whereas the ridged type occurs mostly below ~ -7,000 m (Fig. 1C inlet).

Discussion & conclusions: Based on previous [1,3,6,12] and new observations, it is highly unlikely that the banded terrain is the surface expression of a deeply rooted unit (e.g., truncated layers displaced by ductile deformation during honeycomb formation [13-15]). Instead, the banded terrain seems to be a relatively thin, draping unit that experienced intense, mostly ductile, deformation at relatively shallow depths or at the surface. This viscous behavior, as well as the occurrence of periglacial landforms (e.g., thermokarst-like depressions) [1,3,6], imply a high volatile content in the past. However, its generally elevated thermal inertia (based on THEMIS), along with outcrops and small ejecta containing up to decameter-scale blocks [12], indicate that the banded terrain has since been compacted/cemented and desiccated, probably by katabatic winds. Such winds were suggested to be pervasive in this area [16,17] and likely cause ongoing deflation. Hence, we interpret the ridged type of the banded terrain as degraded version of the creviced type, with the ridges being clastic dikes of material that once filled the crevices. This is in agreement with the ridged type predominantly occurring in the lowest elevations of the unit's extent, where deflation is expected to be more intense [3,17].

Contrary to a previous assessment [1], our observations (band orientations not correlating with the local slopes of modern topography) do not support gravity-driven flow as the source of deformation that resulted in today's banded terrain. Instead, our investigation implies numerous, small-scale, slope-independent stress fields (<10s of km) of different orientations. These stress fields must have sufficed not only to deform the banded terrain, but also to deform superposing crater ejecta in certain locations (e.g., at 57,66°E 35,67°S). Furthermore, as no regional pattern (>10s of km) can be identified within the banded terrain, we suggest that large-scale, regional stress fields had little or no effect on its deformation. "Band hierarchies", i.e., bands overlapping or apparently breaking through each other, indicate multiple phases of deformation, possibly at different strain rates. One possible yet inconclusive formation model for the banded terrain might be a wet-based, subglacial environment, in which ductile material was deformed in stress fields caused by the ice overburden pressure. This pressure acted in conjunction with bed topography as well as zones of variable surging and basal decoupling, resulting in various different strain rates and band arrangements.

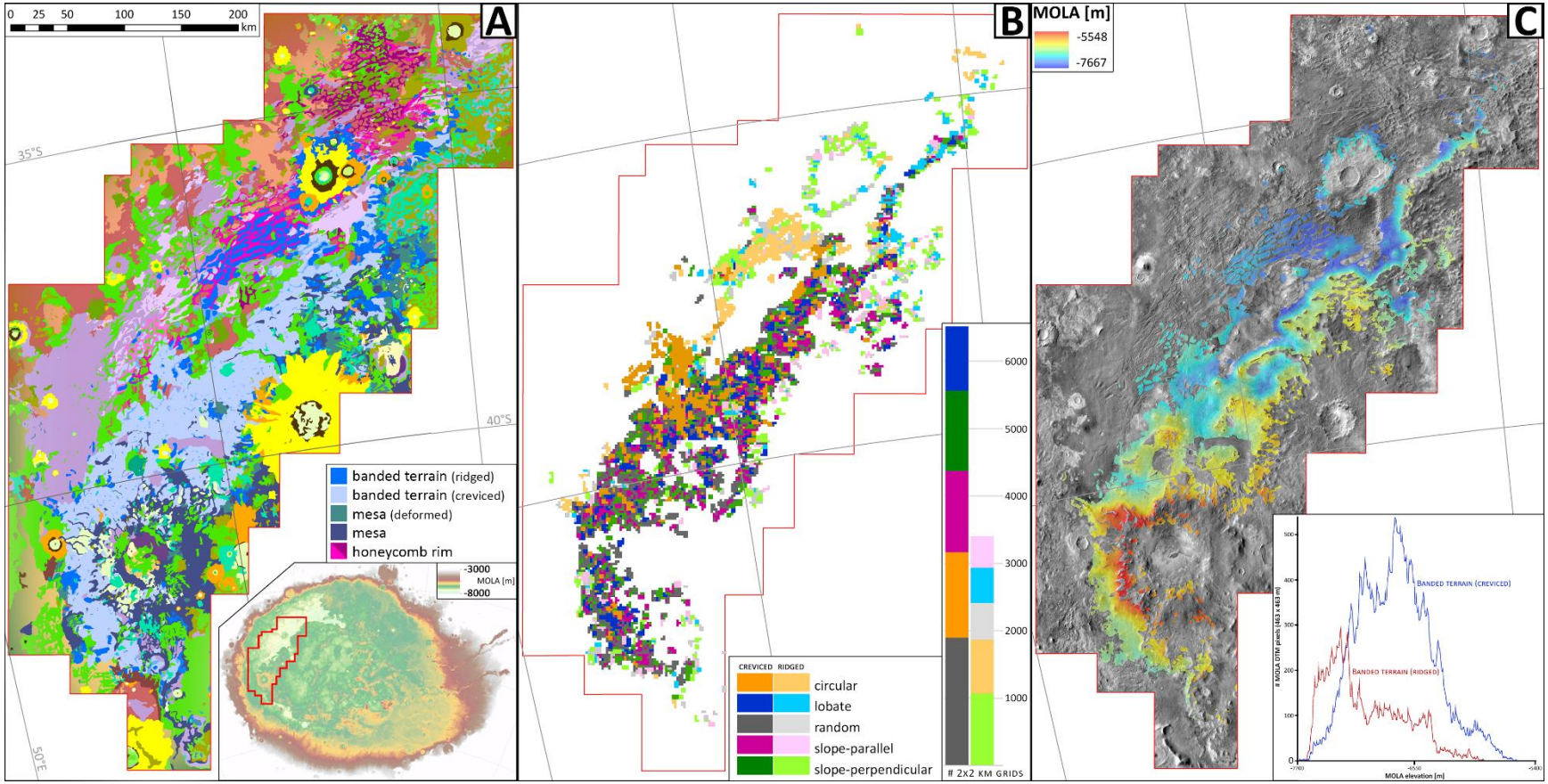

Figure 1: A) Photogeologic map (1:175,000) of a portion of the western Hellas basin floor (see inlet) based on a purpose-built, seamless CTX mosaic. The banded terrain is shown as light and navy blue units; honeycomb cell-separating ridges are mapped as purple units. Dark blue units represent mostly elongate mesas embayed by the banded terrain. **B)** Grid mapping (2x2 km grid size) covering the entire banded terrain (light and navy blue units in (A)). The inlets show the different categories (defined by the banded terrain's relation to the local slope) assigned to grid boxes, as well as their respective abundances, i.e., number of grid boxes (cumulative bar chart). **C)** Topographic analysis of the banded terrain based on MOLA (background THEMIS-IR day mosaic). The inlet shows the elevation distributions of the creviced (blue) and ridged (red) types of banded terrain.

References: [1] Diot, X. et al. (2015) JGR: Planets, 120(12), 2258–2276. [2] Bernhardt et al., (2016) Icarus, 265, 407-442. [3] Bernhardt et al., (2016) JGR: Planets, 121, 714-738. [4] Voelker at al. (2017) PSS, 145, 49-70. [5] Weiss and Head (2017) Icarus, 284, 249-263. [6] Diot et al. (2014) PSS, 101, 118-134. [7] Malin, M. C. et al. (2007) JGR, 112(E5), E05S04. [8] Edwards et al. (2011) JGR: Planets, 116, E10008 . [9] Smith, M. D. et al. (2001) JGR, 106(E10), 23689. [10] McEwen, A. S. (2007) JGR, 112, E05S02. [11] Malin, M. C., & Edgett, K. S. (2010) The Mars Journal, 5, 1–60. [12] Diot, X. (2015) PSS, 121, 36–52. [13] Moore and Wilhelms (2001) Icarus 154, 258-276. [14] Mangold and Allemand (2003) Int. Conf. Mars#3047. [15] Kite et al., (2009) LPSC#1249. [16] Siili, T. (1999) PSS, 47(8–9), 951–970. [17] Howard et al. (2012) LPSC#1105.